Bull Volcanol (1988) 50:119-129

Bulletin of Volcanology

The ground layer of Ata pyroclastic flow deposit, southwestern Japan — evidence for the capture of lithic fragments

Keiko Suzuki-Kamata*

Department of Earth Sciences, Faculty of Science, Kobe University, Nada, Kobe 657, Japan

Abstract. Lithic fragments in the ground layer of the Ata pyroclastic flow deposit, southwestern Japan, were supplied from two different sources. One is the eruptive vent and the other is the basement rock exposed underneath the path of flow. Lithic fragments captured at the eruptive vent gradually decrease in size with distance from the source. Local increases of ML or Md are proportional to increased amounts of captured lithic fragments. The pyroclastic flow eroded basement formations on slopes dipping away from the source, and deposited the lithics within the ground layer on slopes dipping towards the source. The ground layer was found only in the western half of the Ata pyroclastic flow deposit. The absence of the ground layer in the eastern half of the pyroclastic flow deposit is interpreted to result from a selective loss of lithics when the flow traversed a bay or a lake located just east from the vent.

Introduction

Lithic fragments in pyroclastic flow deposits are composed of two kinds of materials. These include material that originated from erosion of the vent, as well as material that was eroded and picked up from the surface during flowage.

Materials eroded from the vent make it possible to estimate the location of the vent. For example, Hildreth and Mahood (1986) demonstrated that the erupting vent migrated to produce several lobes of pyroclastic flows in the Bishop tuff, on the basis that the pyroclastic flow deposits contain different kinds of lithic fragments in different directions around the caldera. Materials eroded and captured during flow are recognized by exposures that include weathered material older than the pyroclastic flow deposit. Similar work by Sakaguchi (1980) and Sakaguchi and Ui (1983) demonstrated that the Tashiro pyroclastic flow in Japan eroded underlying material at topographical ridges, and captured lithic fragments of the basement formation.

The Ata pyroclastic flow deposit in southern Kyushu, Japan, has a coarse, fines-depleted layer at its base that is up to 2 m thick. This layer is interpreted to be a ground layer (hereafter referred to as GL) (Walker et al. 1981) because of the following four reasons: (1) the layer underlies the ordinary part of the Ata pyroclastic flow deposit and is separated from it by a sharp boundary; (2) the layer is fines-depleted, and is rich in lithic fragments and poor in essential fragments; (3) the layer shows evidence of erosion of the basement by the flow; and (4) the layer does not show mantle bedding in spite of good sorting. The fines-depleted layer is probably not an independent pyroclastic flow lobe, because there is less than 10% of juvenile fragments in the material. This is probably too small a fraction of juvenile material for a pyroclastic flow to flow 100 km from the source.

GL was first described by Walker et al. (1981) as the lithic-enriched basal part of the Taupo ignimbrite in New Zealand. They interpreted that GL was emplaced by the strongly fluidized head of the pyroclastic flow. The GL deposit is sharply overlain by the deposit of the remainder of the same flow. The proportion of lithic fragments within a GL is much higher than that of overlying ordinary deposits. Therefore, the lithic fragments in the GL are interpreted to be captured within

* *Present address:* Earthquake Research Institute, University of Tokyo, Yayoi 1-1-1, Bunkyo-ku, Tokyo 113 Japan

the pyroclastic flow when the head of a pyroclastic flow flows over and erodes the wall of the eruptive vent and the ground surface. Component analyses of the lithic fragments contained in the ground layer can give us much information on the degree and mode of erosion by a large-scale pyroclastic flow.

In this paper, grain size analyses and component analyses of lithic fragments for the GL of the Ata pyroclastic flow deposit are carried out and the degree of erosion by a pyroclastic flow is discussed. In addition, the polarity of distribution and the lateral change of lithofacies in the GL of the Ata pyroclastic flow deposit are described. The Ata pyroclastic flow deposit is a good deposit to study because the basal parts of the pyroclastic flow are exposed in many locations at various distances from the source caldera.

Ata pyroclastic flow deposit

The Ata pyroclastic flow deposit is one of the Quaternary large-scale pyroclastic flow deposits in Japan. The limit of its distribution is more than 100 km (Watanabe 1985) away from the centre of the caldera in the southern part of Kagoshima Bay (Fig. 1). The entire rim of the caldera (Fig. 1) is now submerged beneath Kagoshima Bay (Aramaki and Ui 1966; Hayasaka 1982; Suzuki and Ui 1983). Pyroclastic flow plateaus are present only along the eastern shore of the bay, adjacent to the caldera. The maximum thickness of Ata pyroclastic flow deposit is 100 m. The age of eruption is estimated to be 80 000–85 000 years B. P., based on the tephrochronology of the co-ignimbrite ash deposit (Machida 1984). The magma-equivalent volume of the Ata pyroclastic flow deposit is more than 50 km^3 (Aramaki and Ui 1966; Suzuki 1983).

The deposit is composed of lower non-welded facies and upper-welded facies. No evidence of an erosional time break is confirmed between these two facies. The lower, non-welded facies is found only in the areas east and southeast of the caldera, where it is thin and stratified. Surge deposits with a wave length of several metres are lo-

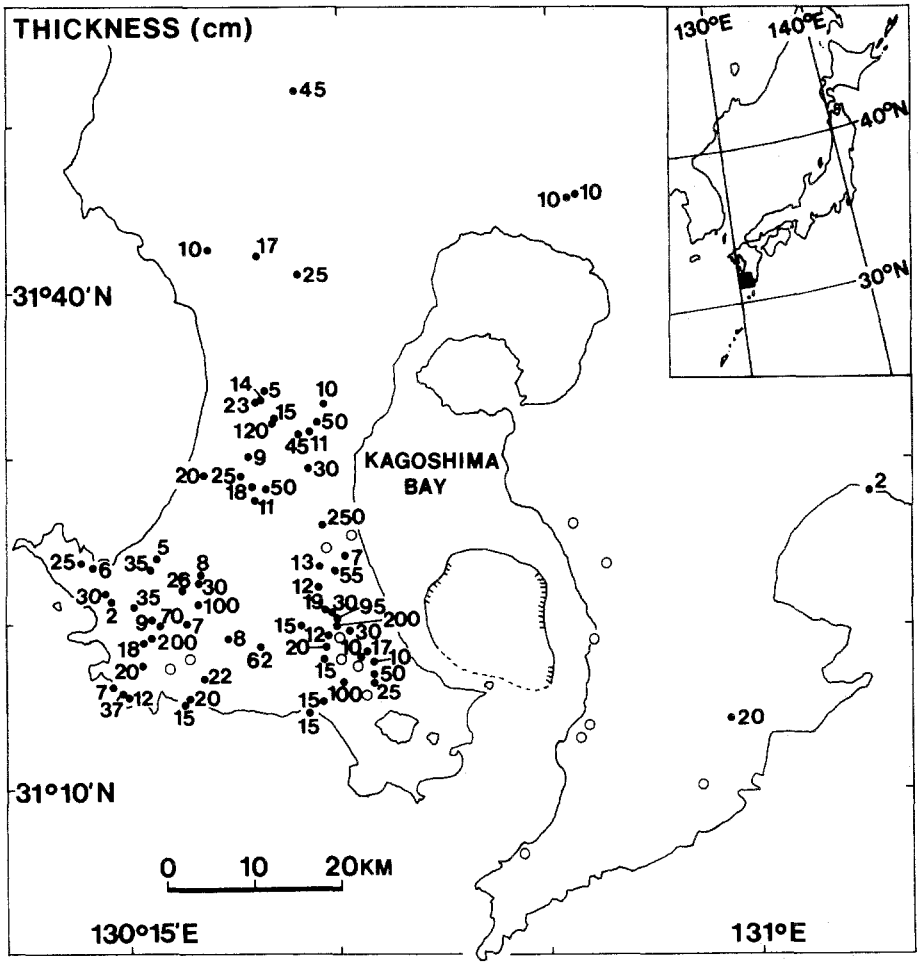

Fig. 1. Map showing the thickness of the ground layer (GL) in the Ata pyroclastic flow deposit. The thickness is given in centimetres. The estimated location of the rim of the source caldera is indicated by the *solid* and *dashed lines* (Hayasaka 1982). *Open circles* show localities where GL was not found at the base of the Ata pyroclastic flow. The *inset map* shows the location of the area studied. Distribution of the GL is limited mostly to the western side of the caldera. No systematic change of thickness is observed

cally observed in the lower facies. Upper welded facies are recognized all around the caldera. The deposit overlies a fallout tephra made of an alternation of ash fall containing accretionary lapilli and plinian pumice.

The GL is commonly found at the bottom of the upper welded facies (Fig. 2). The GL is distributed mainly west of the source caldera (Fig. 1). No GL is identified in the area east of the caldera. No systematic change of thickness with distance from the source caldera is recognized (Fig. 1). The thickness of the GL is variable even within an exposure, and generally increases downwards on a gentle slope of the pre-flow channel.

GL exposures usually are massive, coarse-grained, fines-depleted and rich in lithic fragments. However, the lithology of the GL changes at the northwestern distal areas. Instead of the usual GL, a fine-ash layer accompanied by a lensoid crystal-rich part is locally present at the basal part of the Ata pyroclastic flow deposit (Fig. 3). The presence of the crystal-rich lenses and the sharp boundary with the upper ordinary part of the pyroclastic flow deposit indicates that the fine-ash layer is not the fines-rich layer 2a of Sparks et al. (1973). Both the fine-ash part and the crystal-rich part are composed of well-sorted materials. Since this deposit contains carbonized wood and clots of soil, and is in the same position stratigraphically as the main GL, it is interpreted to be of pyroclastic flow origin and a lateral facies variation of the GL.

Grain size

Grain size and component analyses of lithic fragments were made for the GL of the Ata pyroclastic flow deposit. The GL was identified and sampled at 72 exposures (Fig. 1). The distance from the centre of caldera to the nearest sampled exposure is 18 km, and to the farthest sampled exposure is 65 km.

The average of the maximum diameters of the three largest lithic fragments in the GL (hereafter referred to as ML) was determined at each exposure (Fig. 4). ML generally decreases with increasing distance from the source, but a local increase of ML is observed in the northwestern distal area (Fig. 4).

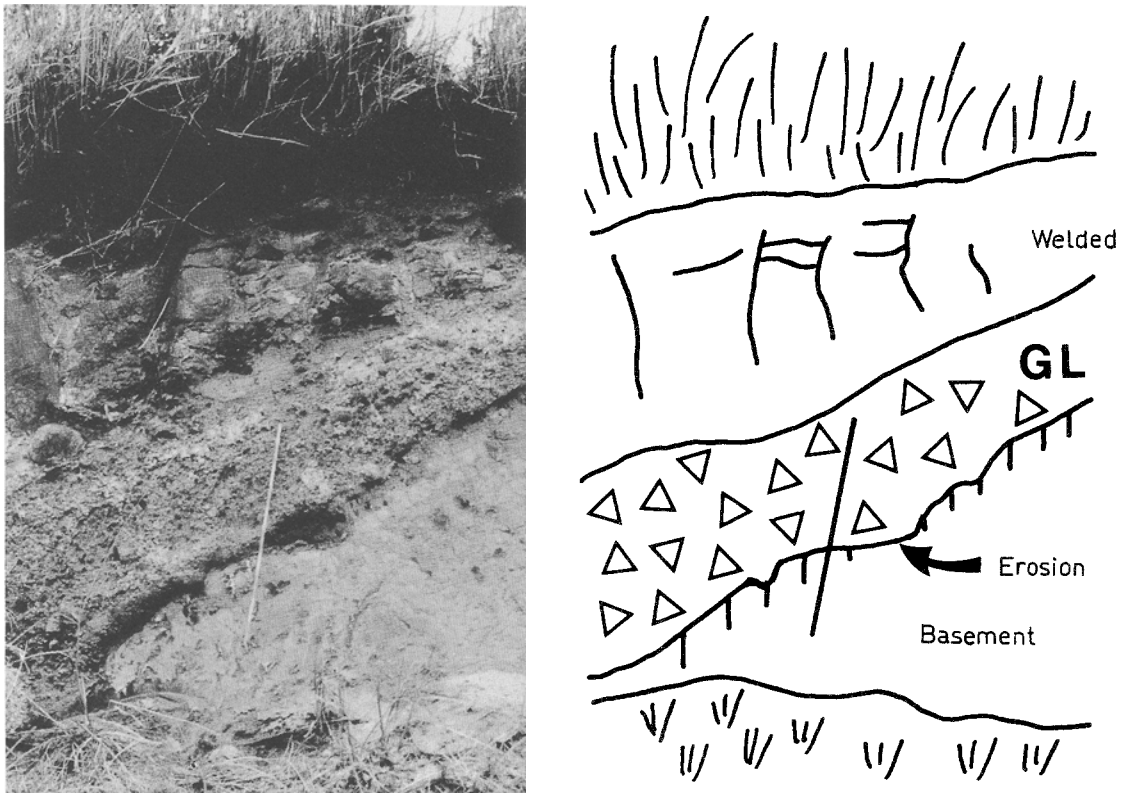

Fig. 2. The GL overlies the weathered surface of basement flysch-type sedimentary formation. Scale is 1 m in length. The weathered surface was locally eroded by the GL

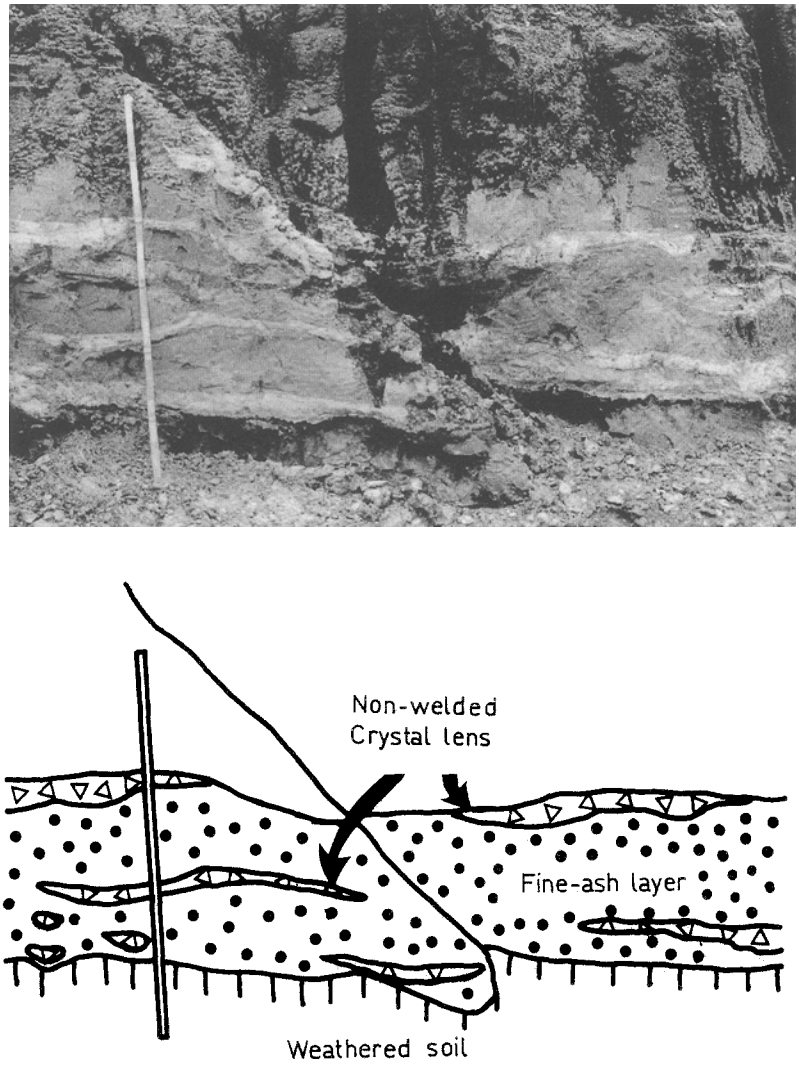

Fig. 3. A fine-ash layer, including a crystal-rich lensoid, overlies the weathered soil of the distal area. Scale is 1 m in length

Thirty-seven fresh GL samples of 1–2 kg each were collected from 33 exposures. The samples were sieved into ten intervals from −5 to +4 phi (32 to 1/16 mm). Most of the GL samples are coarse-grained (Md-phi < −0.4), and are poor in fine ash smaller than 1/16 mm in diameter (*solid line* in Fig. 5) as compared with samples from the ordinary non-welded Ata pyroclastic flow deposit (*dashed line* in Fig. 5). This feature is similar to that of the Taupo ignimbrite described by Walker et al. (1981). However, a sample from the distal area (*dotted line* in Fig. 5) contains 44% fine ash, and is well sorted. Consistent with the ML trend, the median diameter (Md) of GL generally decreases with increasing distance from the source. However, locally some low Md values were obtained at 18–30 km distance from the source (Fig. 6), and some high Md values were obtained at 30–50 km distance from the source (Fig. 6).

Source of GL material

The proportions of each kind of lithic fragments were measured for three sieved fractions, namely, over 32 mm in diameter, between 32 and 16 mm, and between 16 and 8 mm. Andesites, sedimentary rocks which may correspond to the basement flysch-type sedimentary formation (Shimanto Super Group), tuffs derived from underlying pyroclastic flow deposits, well-sorted fine-ash deposits, granite, granite porphyry, and hydrothermally altered volcanic rocks were identified. These lithic fragments were separated according to rock type (component analysis) for approximately 500 clasts for fractions between 16 and 8 mm in diameter, 100 clasts between 32 and 16 mm and 10 clasts over 32 mm respectively.

The ratio of lithic components is shown by the weight percentage of each fraction (Fig. 7). The

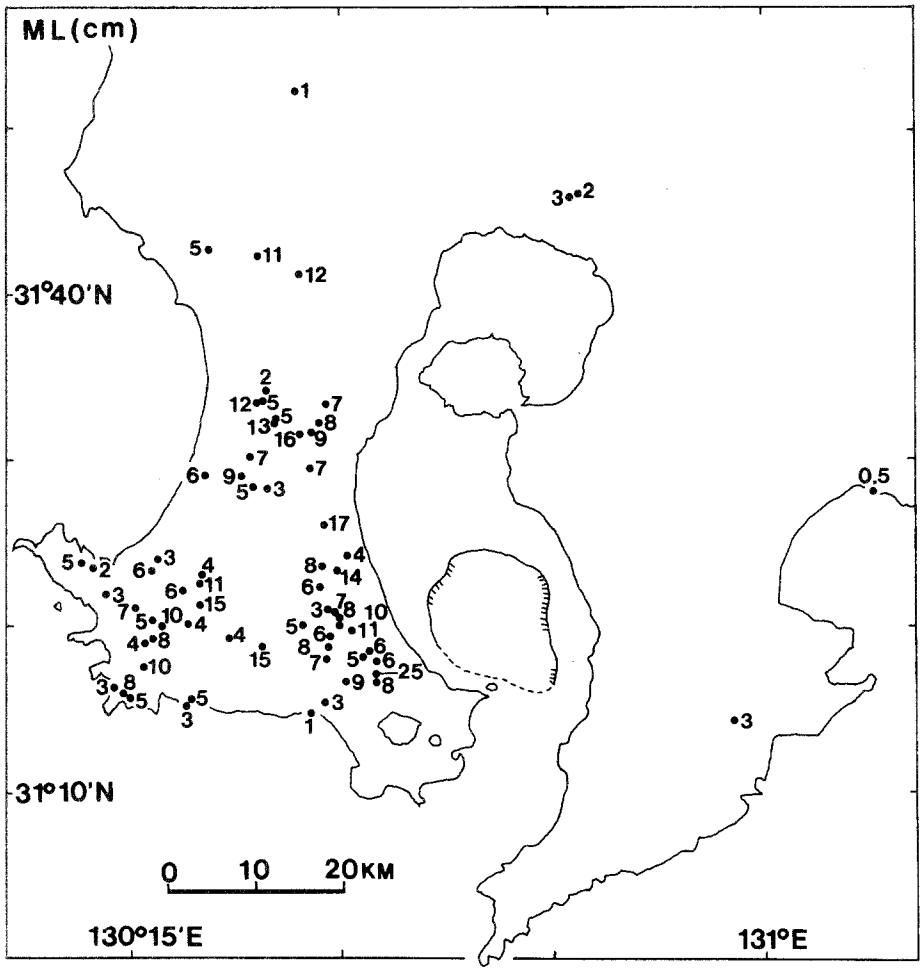

Fig. 4. Map showing the average maximum diameter of the three largest lithic clasts (ML) in an exposure of the GL. ML is given in centimetres. ML shows no systematic change with distance from the caldera

correlation of lithics in the GL with the basement formations is useful to estimate the source of GL material. Cretaceous sediments are predominantly in the bedrock in the northwestern area at a distance of 15–48 km from the centre of the caldera. Cretaceous sediments are exposed at the sampling sites of G20, G21, G14, G29, G28, G5, G26 and G27 (Fig. 7). However, the major lithic component of GL in these localities is porphyritic augite-hypersthene andesite (Fig. 7). Because there are no exposures of such andesites in areas between these sampling sites and the source calderas, porphyritic augite-hypersthene andesite probably was supplied from the eruptive vent. Andesite and underlying flysch-type sediments are exposed in eastern and western areas along the bay adjacent to the caldera, suggesting that not only andesite but also flysch-type sediments are distributed around the source caldera. The interpretation that porphyritic augite-hypersthene andesite was exposed at the eruptive centre is consistent with the conclusion of Aramaki and Ui (1966).

The ratio of andesite captured at the eruptive vent was plotted versus distance from the centre of the estimated caldera. The weight percentage of porphyritic andesite in the grain-size ranges of 16–8 mm *(open circle)* and 32–16 mm *(solid circle)* decreases with increasing distance from the source (Fig. 8). The andesite disappears at points approximately 45 km northwest from the centre of the caldera. On the contrary, lithics of aphyric andesite in both grain-size ranges appear only in the north-northwestern area furthest from the vent, instead of lithic fragments of porphyritic andesite. This aphyric andesite is widely exposed in the area at the north end of peninsula as a basement formation. Andesitic lithic fragments contained in GL of G33, G10, G25 and G32 are all aphyric andesite. The decreasing ratio of the porphyritic andesite component in the GL suggests that lithics of porphyritic andesite captured at the eruptive

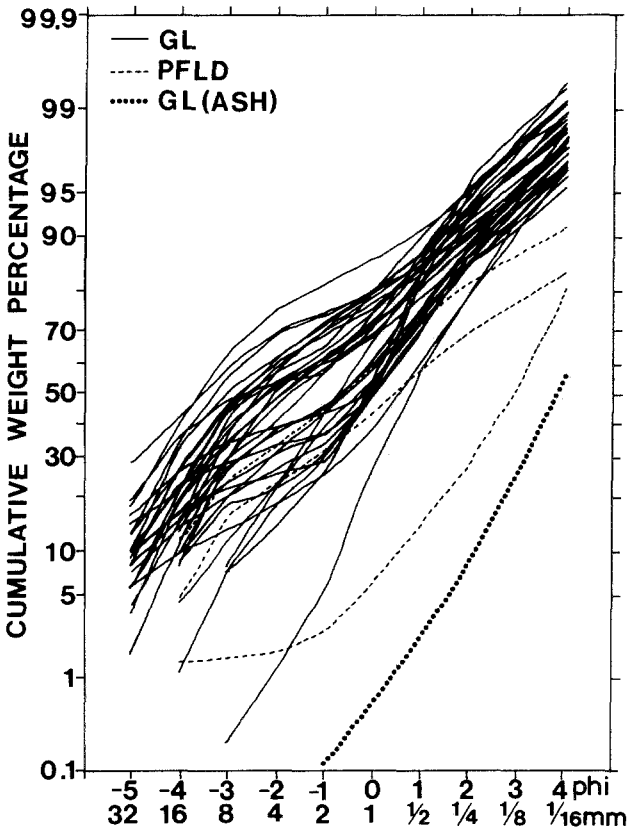

Fig. 5. Representative probability curves of GL samples showing the cumulative weight percentage by *solid lines*. The *dashed lines* (PFLD) are representative typical samples of the non-welded portion of the Ata pyroclastic flow deposit for comparison. The *dotted line* (GL(ASH)) is the sample of the fine-ash layer in the distal area of the GL. Finer ash smaller than 1/16 mm in diameter is low in the GL, and enriched in the fine-ash layer

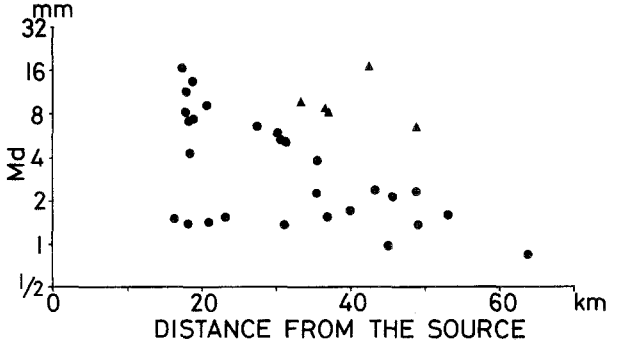

Fig. 6. Variation of median diameter (Md) of clasts in the GL plotted distance from the centre of the caldera. Md values of clasts derived from both vent and flowage path show a decreasing trend with increasing distance from the source. Some locally high Md values *(solid triangles)* were obtained at 30–50 km distance from the source, reflecting coarse-grained lithics derived from local basement formations

vent were gradually deposited in the GL, at the same time as new lithics were captured by the pyroclastic flow from the underlying ground surface. This process is best shown in the area northwestwards of the vent, where similar rocks of porphyritic andesite are not exposed as a basement formation.

The origin of lithic fragments in the GL during flowage was interpreted from the component analyses of sieved samples (Fig. 7). Coarser lithic components at some localities reflect the basement geology close to sampling sites. On the other hand, finer lithic components are mixtures of locally-derived and vent-supplied materials. For example, all lithic fragments larger than 32 mm in diameter at three exposures 19–36 km away from the centre of the caldera (G2, G3, G15 of Fig. 7) are composed of sedimentary rocks, tuffs and hydrothermally altered rocks respectively. Those rocks are exposed in the areas close to each sampling locality. Finer lithic fragments at the same exposures include vent-supplied andesites as well as the above-mentioned lithic fragments. Lithic fragments larger than 16 mm in diameter at an exposure 43 km away from the source (G13 in Fig. 7) are sedimentary rocks, and those larger than 8 mm in diameter at an exposure 46 km away from the source (G7 in Fig. 7) are composed of granite porphyry. Both sedimentary rocks and granite porphyry were also captured at areas close to the sampling locality. Thus, larger lithic fragments tend to be captured at the area close to the sampling locality and smaller lithic fragments are carried from the vent. At areas farther from the caldera, finer lithic fragments also are to be captured primarily in the area close to the sampling locality.

A local increase of ML (Fig. 4) was recognized at several sampling sites west- to northwest of the caldera (G12, G4, G6, G5, G33, G10 of Fig. 7). GLs at these localities are mainly composed of basement formations exposed around the sampling localities (Fig. 7). ML is enhanced due to the capture of coarser lithic clasts of basement formations close to the sampling localities. Md also shows a local increase and decrease in proportion to ML (Fig. 6). This increase is explained by the same process as the increase in ML.

The effect of topographical barriers on the lithic population was checked by using a set of samples collected at a topographical ridge which is located radially away from the source caldera (G15, G16, G18 in Fig. 7) and within 1 km span (Fig. 9). This area is located approximately 15 km away from the centre of the caldera. Md is larger on the

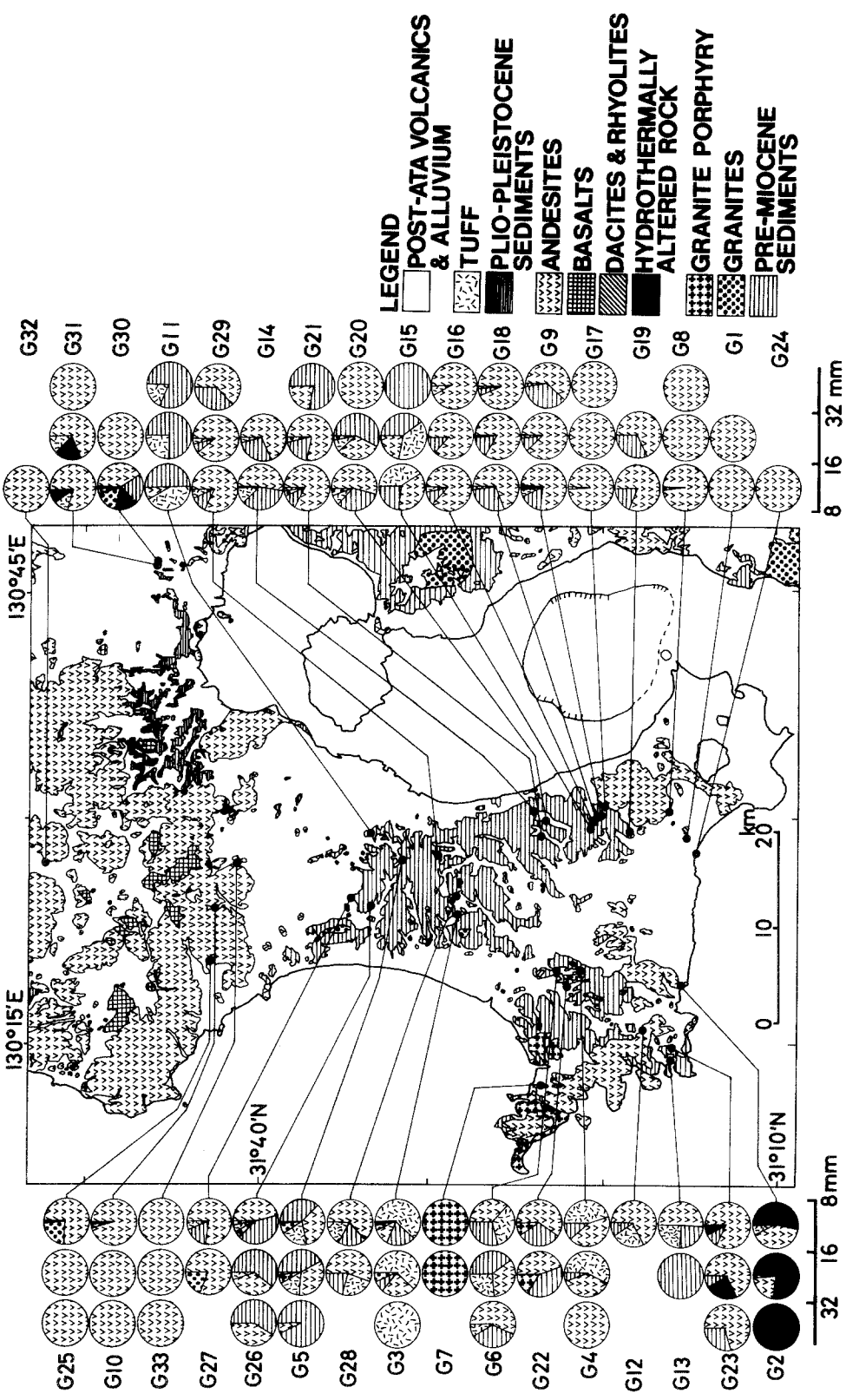

Fig. 7. Map showing the basement geology and results of component analyses of the GL. Component analyses were made for the three grain size ranges, 8–16 mm (−3 to −4 phi), 16–32 mm (−4 to −5 phi) and over 32 mm (> −5 phi). For detailed discussions, see text

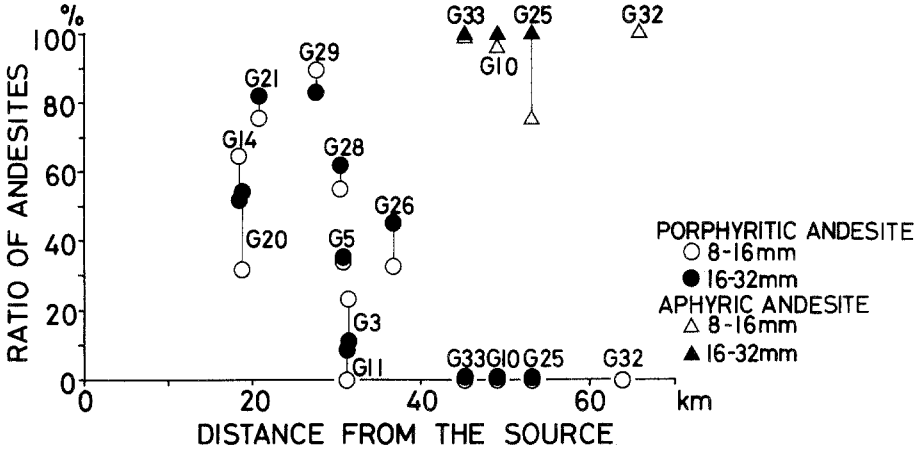

Fig. 8. Relationship between the weight percentage (wt%) of the andesite fragments in each fraction of the GL and the distance from the source caldera. A pair of *open* and *solid circles* represents wt% for porphyritic augite-hypersthene andesite for grain size ranges 8–16 mm and 16–32 mm in diameter. Probable errors of each components at the 95.4% confidence levels are within 5% for clasts whose grain size range is 8–16 mm in diameter, and within 10% for clasts whose grain size range is 16–32 mm. *Open* and *solid triangles* represent wt% for aphyric andesite of the same grain size ranges. Weight percentage of the porphyritic andesite decreases with increasing distance from the source, and reaches zero at approximately 45 km away from the centre of the caldera

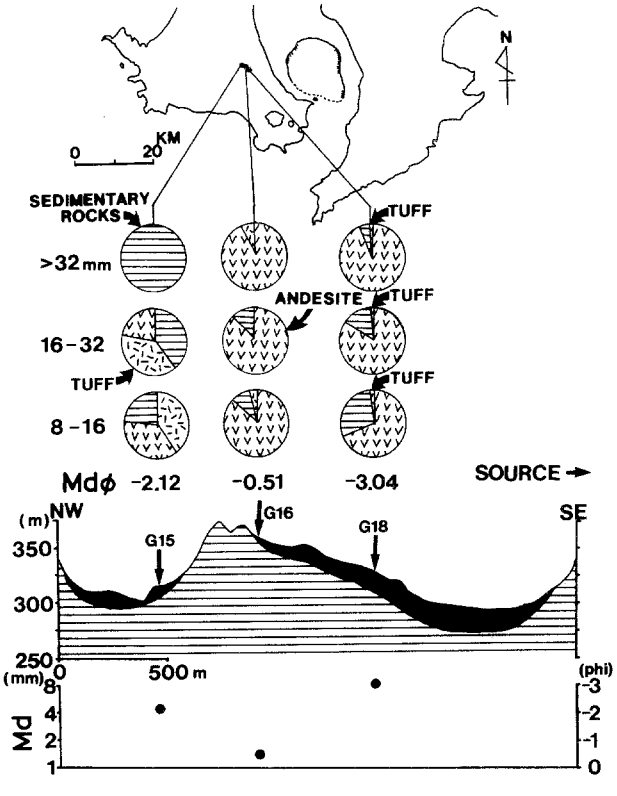

Fig. 9. Diagram showing the result of component analysis of the GL at the lee- and stoss-sides of a topographical barrier. The result suggests that the pyroclastic flow deposits lithics as a GL on the stoss-side slope (G18, G16), and captures new lithic fragments from the surface on the lee-side slope (G15)

lower part of the slope (G18, G15 of Fig. 9) than on the upper part (G16). The lithic component on the source-facing slope mostly consists of porphyritic andesite captured at the vent. Flysch-type sediments are scarce amongst the lithics (G16 and G18 in Fig. 9). However, flysch-type sediments are abundant behind the topographical barrier (G15 in Fig. 9). This indicates that new lithics are captured from the surface on the lee-side slope (Fig. 10), suggesting that the pyroclastic flow

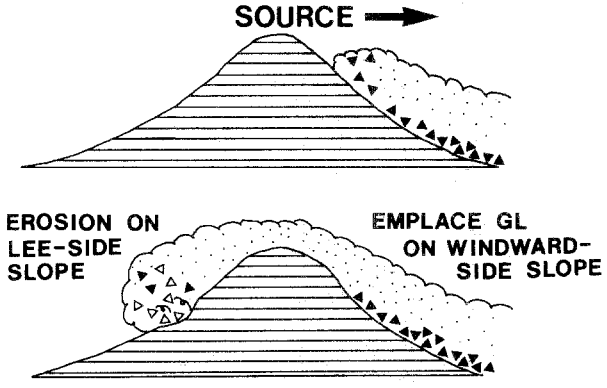

Fig. 10. Schematic diagram to explain the change of lithic abundance on the stoss- and lee-side slopes. The pyroclastic flow deposits lithic fragments on the stoss-side slope, whereas it captures basement fragments on the lee-side slope

eroded basement rocks more actively on the descending slope than on the climbing slope.

Recently, Hildreth and Mahood (1986) and Potter and Oberthal (1987) demonstrated propagations of vents of Bishop tuff and Bandelier tuff by means of areal variations in compositions of lithic fragments. Their arguments are based on the premise that the diversity of basement rocks around the vent may directly influence the components of lithic fragments measured on outcrops. However, the result of this study indicates that lithic fragments do not necessarily originate from the vent, but are commonly captured during flowage, especially in the distal areas. Therefore, estimating the location of vent using the techniques of Hildreth and Mahood (1986) and Potter and Oberthal (1987) is valid only when this capturing effect is negligible.

Lack of GL on the east side of the caldera

The GL of the Ata pyroclastic flow deposit is distributed mainly on the west and north sides of the caldera. The GL is mostly absent on the east-side. Such a distribution pattern is different from the case of Taupo ignimbrite, where GL is found in all directions around the caldera (Walker et al. 1981). Two possibilities are suggested to explain this phenomenon.

The first model is that the vent enlarged westwards and northwestwards during the eruption. The lower non-welded member of the Ata pyroclastic flow deposit is exposed only eastwards and southeastwards of the vent. The distribution of the lower member in the east and southeast of the caldera suggests that the vent was located in the southeastern part of the caldera at the first stage of eruption. If the vent enlarged westwards and northwestwards to supply the large-volume magma extrusion at the time of eruption of the upper member, many lithics might have been supplied selectively westwards and northwestwards from the vent, which corresponds to the newly enlarged direction. However, GLs also do not exist at localities northeastwards and southwards from the caldera, which are located radially away from the enlarged caldera. This is inconsistent with the first model, because even if the vent enlarged westwards and northwestwards, GLs should exist in every direction except for eastwards and southeastwards.

The second model is that the flow itself originally extended radially all around the caldera, but lithic fragments were selectively lost where the flow traversed a lake or a bay east of the vent. Walker (1983), Ono and Watanabe (1983) and Ui et al. (1983) have demonstrated that pyroclastic flows may cross the sea. Grain-size analyses and density measurements for the Aso and the Koya pyroclastic flow deposits indicate that loss of lithic fragments possibly occurred because these flows traversed the sea (Ono and Watanabe 1983; Ui et al. 1983), when lithic fragments dropped into the water due to the high density of the lithic material compared with the main body of the pyroclastic flow. The absence of the Ata GL along the present coastline suggests that a bay or a lake existed east of the vent during the eruption, because the GLs exist at the localities 30–45 km distant from the centre of the caldera in the east (Fig. 1), but these are composed of basement rocks eroded locally from the basement. The width of the bay or lake must have been less than 10 km, based on the present topography.

Other facies of the Ata pyroclastic flow deposit suggest the presence of a body of water near the vent at the beginning of the eruption. The Ata pyroclastic flow deposit contains a lower non-welded member that includes a pyroclastic surge deposit. Its distribution is restricted to the east-southeast of the caldera. In addition, a fine-ash fall deposit that includes accretionary lapilli precedes the climactic eruption. Because water interaction is restricted to the first stage of the eruption, the vent of the Ata pyroclastic flow probably shifted towards the dry area to the west and northwest later. The second model is adopted here as the most persuasive explanation for the lack of the GL to the east side of the caldera.

Origin of the distal fine-ash GL facies

The GL in Taupo ignimbrite is massive, rich in lithic fragments, and poor in fine ash throughout (Walker et al. 1981). However, at the distal area of the Ata pyroclastic flow deposit (Fig. 3) a fine-ash layer that includes a lensoid crystal-rich part is recognized as a lateral facies variation of the normal massive and well-sorted GL.

The fine-ash part of this layer at locality G32 contains 44% of fine ash smaller than 1/16 mm in diameter, and is finer and better sorted than the non-welded pyroclastic flow deposit (Fig. 5). The crystal-rich part of the same deposit at the same exposure contains only 3% of fine ash smaller than 1/16 mm in diameter, and is composed of well-sorted crystals, pumice and lithic fragments. The layer is identified as GL because it is sharply

overlain by a normal pyroclastic flow deposit and is well-sorted.

The layer closely resembles segregation structures shown in Wilson's (1980, 1984) fluidization experiments. The transformation of the GL to a segregation structure indicates that the gas velocity of the fluidized bed at the flow head decreases in the distal area. It is suggested here that the kind of pyroclastic material emplaced from the moving pyroclastic flow depends on the relationship between the gas velocity of the fluidized bed and the terminal velocity of the pyroclastic material. That is, if the gas velocity of fluidized bed is larger than the terminal velocity of fine ash, a normal fines-depleted GL is formed at the head of the pyroclastic flow. On the other hand, if the gas velocity decreases according to the distance from the source and becomes smaller than the terminal velocity of fine ash, then the GL at the head of the pyroclastic flow forms the segregation structure facies with a fine-ash layer and a crystal-rich lensoid part. The decreasing gas velocity of the fluidized flow head is in harmony with the decrease of ML and Md with distance from the source.

Conclusions

A GL (ground layer) was identified in the Ata pyroclastic flow deposit. The layer underlies the ordinary Ata pyroclastic flow deposit with a sharp boundary, is fines-depleted, rich in lithic fragments, poor in essential fragments, and shows an erosional contact with the underlying basement surface — all features that identify it as a ground layer.

Two sources of material for the GL of the Ata pyroclastic flow deposit are identified. Some of the lithic fragments were captured at the source vent and the remainder were captured from bedrock underneath the path of the flow. Lithic fragments derived from the source vent are dominant in the vicinity of the source caldera. Lithic fragments larger than 8 mm in diameter captured at the vent disappear about 45 km from the centre of the caldera. By contrast, the proportion of lithics captured from bedrock increases away from the source. Locally high proportions of captured lithic fragments produce locally high ML or Md. The erosional process is predominant on the lee-side slope, because the velocity of the pyroclastic flow is increased when the flow descends the slope. The variations in lithic contents discussed here suggest that caution should be used when interpreting the position of a vent using the analysis of lithic fragments in a pyroclastic flow deposit.

The lack of GL east of the caldera is interpreted to result from the existence of a bay or a lake to the east and southeast of the caldera. Loss of lithics probably occurred when the flow crossed the water.

The GL of the Ata pyroclastic flow deposit is similar to the Taupo ground layer in the proximal part, but shows a lateral facies variation in the distal part that consists of a fine-ash layer which includes a crystal-rich lenses. This is interpreted to result from a low gas velocity near the distal end of the flow that was lower than the terminal velocity of the fine ash.

Acknowledgements. This work was done in partial fulfillment of a Ph. D. thesis at Kobe University. The author wishes to express sincere gratitude to T. Ui, H. Glicken, S. Aramaki and H. Kamata for their constructive discussions at the various stages of this work and critical readings of the manuscript.

References

Aramaki S, Ui T (1966) Aira and Ata pyroclastic flows and related caldera depressions in southern Kyushu, Japan. Bull Volcanol 29:29–48

Hayasaka S (1982) Kagoshima Bay as a graben structure. In: Y Matsumoto (ed) Reports on the basement formations and graben structures in Kyushu 1:76–78 (in Japanese)

Hildreth W, Mahood GA (1986) Ring-fracture eruption of the Bishop Tuff. Geol Soc Am Bull 97:396–403

Machida H (1984) The significance of explosive volcanism in the prehistory of Japan. Geol Surv Japan Rep 263:301–313

Ono K, Matsumoto Y, Miyahisa M, Teraoka Y, Kambe N (1977) Geology of the Taketa district. Geol Surv Japan: pp 1–145 (in Japanese with English abstract)

Ono K, Watanabe K (1983) The Aso-4 pyroclastic flow has traversed the sea. Abstract for annual meeting of Geol Soc Japan:307 (in Japanese)

Potter DB, Oberthal CM (1987) Vent sites and flow directions of the Otowi ash flows (lower Bandelier Tuff), New Mexico. Geol Soc Am Bull 98:66–76

Sakaguchi K (1980) The Tashiro pyroclastic flow deposit, Ohsumi Peninsula, Japan. Master thesis of Kobe University: pp 1–42 (in Japanese with English abstract)

Sakaguchi K, Ui T (1983) Capture of lithic fragments during flowage of a pyroclastic flow — a case study in the Tashiro pyroclastic flow, southern Kyushu, Japan. Bull Volcanol Soc Japan 2nd ser 28:317–320 (in Japanese)

Sparks RSJ, Self S, Walker GPL (1973) Products of ignimbrite eruptions Geology 1:115–118

Suzuki K (1983) Flow and emplacement mechanisms of a large-scale pyroclastic flow. Ph. D. Thesis Kobe University:pp 1–193

Suzuki K, Ui T (1983) Factors governing the flow lineation of a large-scale pyroclastic flow — An example in the Ata pyroclastic flow deposit, Japan. Bull Volcanol 46:71–81

Ui T, Metsugi H, Suzuki K, Walker GPL (1983) Flow lineations of Koya low aspect-ratio ignimbrite, south Kyushu, Japan. EOS 64:45

Walker GPL (1983) Ignimbrite types and ignimbrite problems. J Volcanol Geotherm Res 17:65–88

Walker GPL, Self S, Froggatt PC (1981) The ground layer of the Taupo ignimbrite: A striking example of sedimentation from a pyroclastic flow. J Volcanol Geotherm Res 10:1–11

Watanabe K (1985) Ata pyroclastic flow deposit in the Hitoyoshi Basin, Kumamoto Prefecture, Japan. Mem Fac Education Kumamoto University Natural Science 34:55–62 (in Japanese)

Wilson CJN (1980) The role of fluidization in the emplacement of pyroclastic flows: an experimental approach. J Volcanol Geotherm Res 8:231–249

Wilson CJN (1984) The role of fluidization in the emplacement of pyroclastic flows, 2: Experimental results and their interpretation. J Volcanol Geotherm Res 20:55–84

Received October 21, 1987/Accepted October 27, 1987